

# Selective Gas-Phase Depletion of Chemical Contaminants in Dissolved Organic Matter Increases Compositional Coverage by FT-ICR Mass Spectrometry

Published as part of *Journal of the American Society for Mass Spectrometry special issue "Sanibel: Mass Spectrometry for Complex Mixtures in Energy and the Environment"*.

Chad R. Weisbrod,\* Amy M. McKenna, and Christopher L. Hendrickson



Cite This: <https://doi.org/10.1021/jasms.4c00261>



Read Online

ACCESS |



Metrics & More



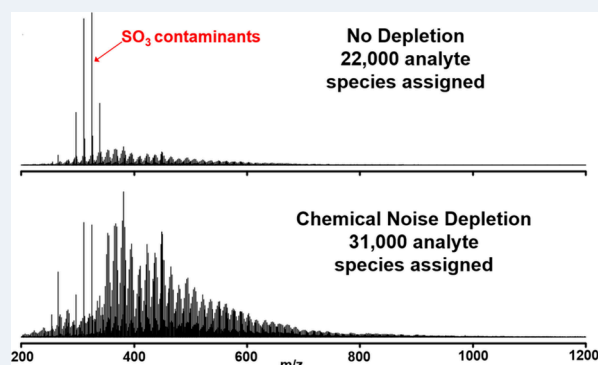
Article Recommendations



Supporting Information

**ABSTRACT:** Fourier transform ion cyclotron resonance mass spectrometry of dissolved organic matter (DOM) extracted from environmental samples provides molecular speciation that enables visualization of compositional trends in the fate and cycling of biogenic and anthropogenic organics. Often, chemical contamination is introduced during field sampling (i.e., remote locations, cannot use glass). Further, preconcentration of DOM by solid-phase extraction often results in chemical contamination. When chemical noise is a dominant fraction of the ion signal, mass spectral performance is degraded by reduction of the ion trap analyte accumulation capacity and enhanced ion cloud dephasing during ICR detection. We have developed gas-phase ion depletion of unwanted chemical contaminants during ion injection into the linear RF ion trap of the hybrid linear ion trap 21 T FT-ICR mass spectrometer that improves detection of analytes by removing unwanted chemical noise. We demonstrate improvements in signal-to-noise ratio, dynamic range, and the number of observed analytes in dissolved organic matter samples that results in a 40–100% increase in the number of identified analytes. In many cases, the number of peaks observed per nominal mass more than doubles over select  $m/z$  regions. This gas-phase “clean-up” can salvage precious samples challenged by sampling location, sample volume, or collection protocols that cannot be avoided and maximizes the compositional information obtained. Further, this approach is generalizable and extendable to any hybrid linear ion trap instrument platform (e.g., LTQ-Orbitrap or linear ion trap-TOF). We highlight the power of gas-phase depletion with electrospray ionization, but this method is also applicable to other ionization modes.

**KEYWORDS:** *Fourier transform ion cyclotron resonance, organic matter, DOM, linear alkyl sulfonates, natural organic matter, linear ion trap MS, complex mixture analysis*



## INTRODUCTION

Chemical noise (i.e., signals observed from sample contamination rather than analytes of interest) is a ubiquitous and confounding problem throughout analytical chemistry. Sulfonate contamination is commonly observed in environmental samples submitted to the Maglab ICR facility but is especially problematic for water samples that seek to track and understand organic carbon cycling in the environment. These compounds are leached into water samples through plastics, tubing, filters, and connectors used in sampling protocols applied in field sites that study extreme environments (e.g. arctic ice sheets, glacial rivers and lakes, and offshore ocean sampling), where cleaner sampling techniques are virtually impossible. Samples collected in extreme environments and far-flung locales are expensive and sometimes even considered “once in a lifetime” collections. Regardless,

recollection of samples that have been deemed contaminated is often not possible. Therefore, any methodology which enables the reduction or elimination of sample contamination is extremely advantageous.

Alkylbenzenesulfonates are anionic surfactants composed of a hydrophilic sulfonate headgroup and a hydrophobic alkylbenzene tail and are some of the oldest and most widely used synthetic detergents. These compounds are often

**Received:** June 14, 2024

**Revised:** September 4, 2024

**Accepted:** September 9, 2024

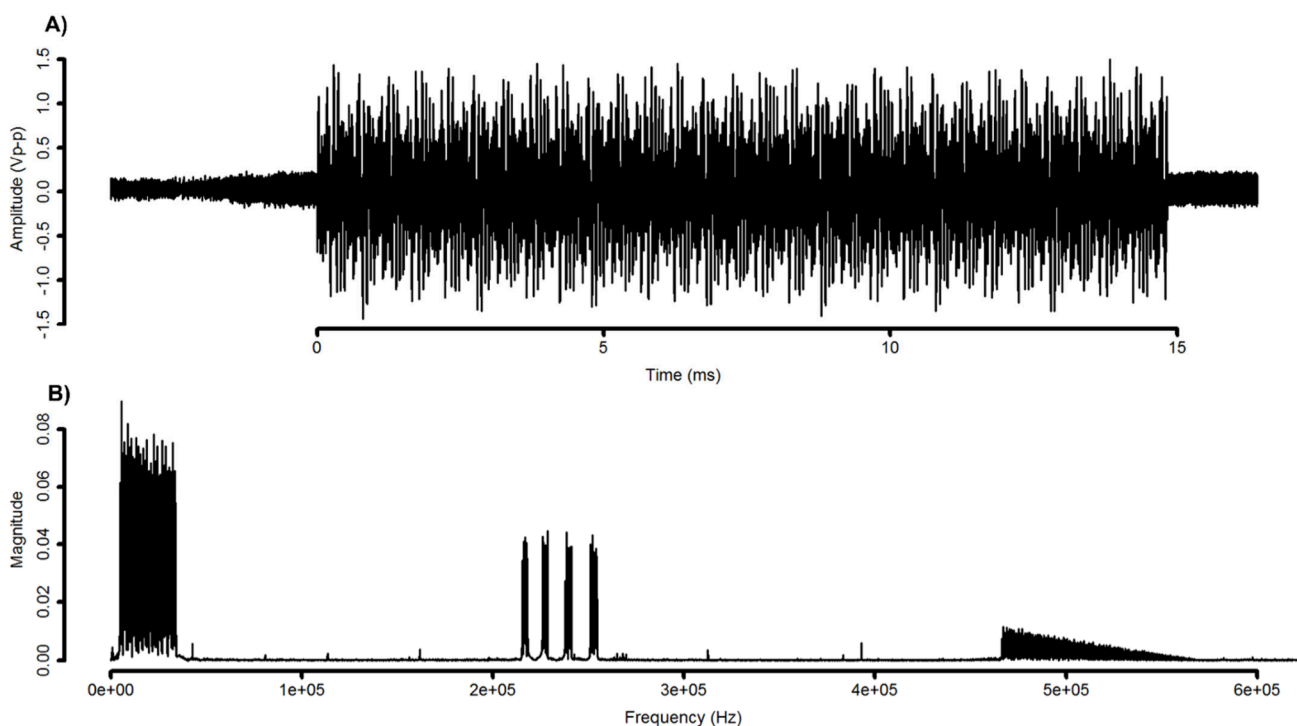


**Figure 1.** (A) Broadband ion depletion waveform acquired prior to amplification and coupling to the x-rod segments of the linear RF ion trap. (B) Fourier transform of the time-domain signal from panel A illustrating the frequency components present within the ion depletion waveform. Of note are the four depletion regions of interest between 220 and 260 kHz. These regions correspond directly to ion frequencies of  $m/z$  297.08, 311.08, 325.08, and 339.08 with a width of 5 Da. The ion trap was set to  $Q = 0.250$ .

accidentally introduced into water samples due to widespread use of plastics and reusable sampling containers. They often appear as a suite of  $\text{SO}_3$  peaks as shown in Figure S1. Several natural organic matter (NOM) studies by FT-ICR MS report highly abundant peaks at  $m/z$  311, 325, and 339, which are identified as  $\text{SO}_3$  compounds and attributed to alkylbenzenesulfonates.<sup>1–7</sup>

Mass spectrometers are unique in the ability to remove unwanted species selectively from a complex sample matrix based on the mass-to-charge ( $m/z$ ) ratio of the unwanted species. In fact, a mass resolving quadrupole selectively purifies the incoming ion beam by allowing only the desired  $m/z$  ions to transmit. Selective broadband filtering approaches have previously been reported but have not been robustly applied in the literature. McLuckey et al. were among the first to demonstrate this approach with both single frequency resonant ejection<sup>8</sup> and tailored waveforms.<sup>9</sup> Bruce et al.<sup>10</sup> applied “colored” noise waveforms to peptide samples and simultaneously enriched analyte signal while removing unwanted species during ion accumulation inside the ICR cell. Another application highlights the selective ejection of abundant species in DREAMS, dynamic range expansion applied to mass spectrometry (DREAMS).<sup>11</sup>

Often, unwanted chemical contaminants such as alkylbenzenesulfonates are the most abundant species in the mass spectrum, due to their high ionization efficiency compared to DOM in negative-ion electrospray ionization, the most widely used ionization mode for DOM FT-ICR MS. Highly selective and efficient removal of these species is possible in the gas phase, within the mass spectrometer. Application of a  $m/z$ -dependent “depletion” waveform during ion injection into the linear RF ion trap on the front-end of the 21 T FT-ICR mass spectrometer ejects most of the unwanted contaminant ions.

When applied to dissolved organic matter analysis, depletion “clean-up” of a water sample facilitates collection of a larger population of desirable analyte ions, which results in a 40–100% increase in the number of detected compounds. The analytical advantages of this approach are demonstrated on several NOM samples of varying ratios of contamination ranging from ~10:1–100:1 (contaminants:analyte). Improvements were observed in mass measurement accuracy, number of detected and identified compounds, expansion in compositional classes observed, and improved number of detected peaks per nominal mass. This method can be applied to selectively remove a user-defined list of  $m/z$  values that can be curated through prescreen analysis of analytical and field blanks.

## EXPERIMENTAL METHODS

**Sample Preparation.** Water samples were acidified, and solid-phase extracted with Bond-Elut PPL columns (Agilent Technologies Inc., Santa Clara, CA) based on previous protocols.<sup>12</sup> HPLC grade methanol was purchased from JT Baker Chemical Company (Phillipsburg, PA). We have selected a few representative samples submitted through the NHMFL ICR facility user program to highlight the applicability of gas-phase depletion to a range of chemical contamination detected in negative-ion electrospray ionization.

**Synthesis and Application of Chemical Noise Depletion Waveforms.** Waveform synthesis was achieved using a custom ITCL script, which permits the synthesis of a broadband waveform with multiple depletion regions (up to ten in our implementation, but the number of regions is adjustable). Each depletion region features independent variables for center  $m/z$ ,  $m/z$  width, and waveform amplitude. The user must possess a priori knowledge of chemical

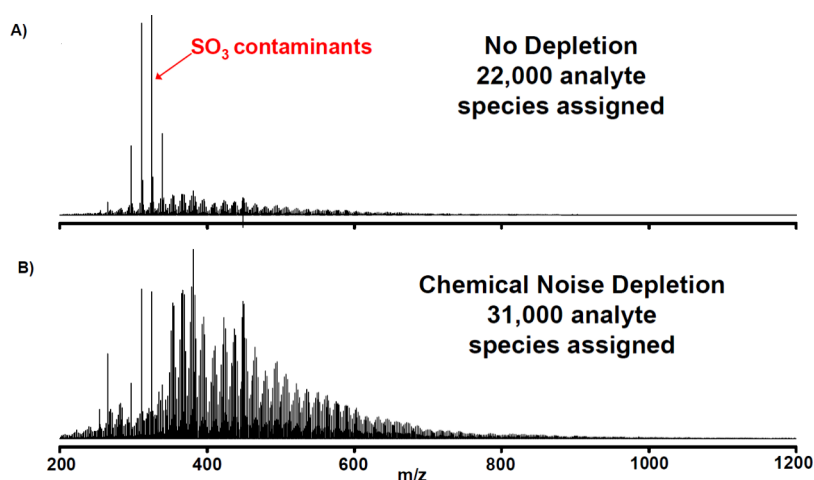


**Figure 2.** (A) Broadband FT-ICR mass spectrum of DOM that contains significant contamination by sulfonate ( $\text{SO}_3$ ) based detergent. The spectrum is the average of 100 transient acquisitions. (B) Broadband FT-ICR mass spectrum of the same sample with a chemical noise depletion waveform applied to eject the unwanted sulfonate contaminant species (average of 100 transient acquisitions). The ion signal attributed to the chemical contaminants is suppressed by nearly 1 order of magnitude.

contaminants expected, and these masses are then defined by the user for waveform synthesis. Often these contaminants are identified through analysis of analytical blanks. Application of the waveform is accomplished via the standard commercial Velos-Pro dual cell linear RF ion trap hardware for arbitrary waveform synthesis and amplification. The waveform is applied to the x-rod set across all three linear segments (front, center, and back) via the arbitrary waveform output device, analogous to the application of ion isolation and ion injection waveforms. In fact, it can be thought of as a “modified” injection waveform. The ion frequency to  $q$ -value calibration performed routinely for ion isolation waveforms is utilized to ensure the depletion waveform frequency components are properly calibrated to the measured  $m/z$  values. Figure 1 shows a scope capture of the broadband ion depletion waveform and the accompanying Fourier transform to reveal the frequency components. Frequency is inversely proportional to  $m/z$  in the linear RF ion trap such that the low frequency high power ( $> \sim 30\,000$  Hz) regime represents frequencies corresponding to  $m/z > 2000$ . The depletion waveform is applied for the entire duration of ion injection into the high-pressure cell of the Velos, with typical ionization times between 0.1 and 100 ms. The depletion waveform is applied for a minimum of 4 ms, which represents two full cycles of the waveform looped from beginning to end.

**Mass Spectrometry and Data Analysis.** Ions were generated at atmospheric pressure via micro-electrospray.<sup>13</sup> All samples were analyzed by negative-ion electrospray 21 T FT-ICR MS.<sup>14,15</sup> Ions were initially accumulated in the high pressure cell of a dual-linear RF ion trap (which is where the ion depletion waveform is applied) and subsequently transferred to an external multipole storage device (MSD) (1–5 ms) and ejected axially with  $m/z$ -dependence to mitigate time-of-flight dispersion in transit from the MSD to the ICR cell.<sup>16</sup> Ions were excited to  $m/z$ -dependent radii to maximize the dynamic range and number of observed mass spectral peaks ( $m/z$  150–1500; 32–64%),<sup>17</sup> and excitation and detection were performed on the same pair of electrodes.<sup>18</sup> The dynamically harmonized ICR cell in the 21 T FT-ICR is operated with 6 V trap potentials.<sup>19,20</sup> Time-domain transients of 3.1 s were acquired with the Predator data station (100

transient acquisitions were averaged for all experiments),<sup>21</sup> which handled excitation and detection initiated by a TTL trigger from the Thermo data station.<sup>15</sup> Mass spectra were phase-corrected<sup>22</sup> and internally calibrated with a high-abundance homologous series based on the walking calibration method.<sup>23</sup> For each elemental composition,  $\text{C}_c\text{H}_h\text{N}_n\text{O}_o\text{S}_s$ , the heteroatom class, type (double bond equivalents,  $\text{DBE} = \text{number of rings plus double bonds to carbon}$ ,  $\text{DBE} = C - h/2 + n/2 + 1$ )<sup>24</sup> and carbon number,  $c$ , were tabulated for subsequent generation of heteroatom class relative abundance distributions and graphical relative-abundance weighted DBE versus carbon number images. Peaks with signal magnitude greater than 6 times the baseline root-mean-square (rms) noise at  $m/z$  500 were exported to peak lists, and molecular formula assignments and data visualization were performed with PetroOrg software.<sup>25</sup> Molecular formula assignments with an error  $> 0.5$  parts-per-million were discarded, and only chemical classes with a combined relative abundance of  $\geq 0.15\%$  of the total were considered. All FT-ICR MS data files are publicly available via the Open Science Framework <https://osf.io/spk2h/> at DOI 10.17605/OSF.IO/SPK2H.

## RESULTS AND DISCUSSION

Here, we apply a novel broadband waveform during ion injection which is designed to selectively eject up to ten of the most abundant contaminant species observed within the mass spectrum. Once an  $m/z$  list has been curated, we utilize selective ejection with multiple resonant frequencies to simultaneously remove selected  $m/z$  during ion accumulation, which is similar in principle to other approaches.<sup>8–11</sup> Though synthesis and application of the waveform is automated via instrument control programming language, a priori knowledge of the contaminant  $m/z$  values are required input for this new instrument function.

On the basis of analysis of analytical field blanks, contaminant peaks were identified as sulfonate contaminants ( $\text{O}_3\text{S}$ , DBE value of 4), with signal magnitude more than 10 times that of the analyte. Figure 1 shows the depletion waveform applied to a series of four dominant sulfonate contaminant species (at  $m/z_{1-4}$  297.08, 311.08, 325.08, 339.08) across a 5 Da width in the linear ion trap mass

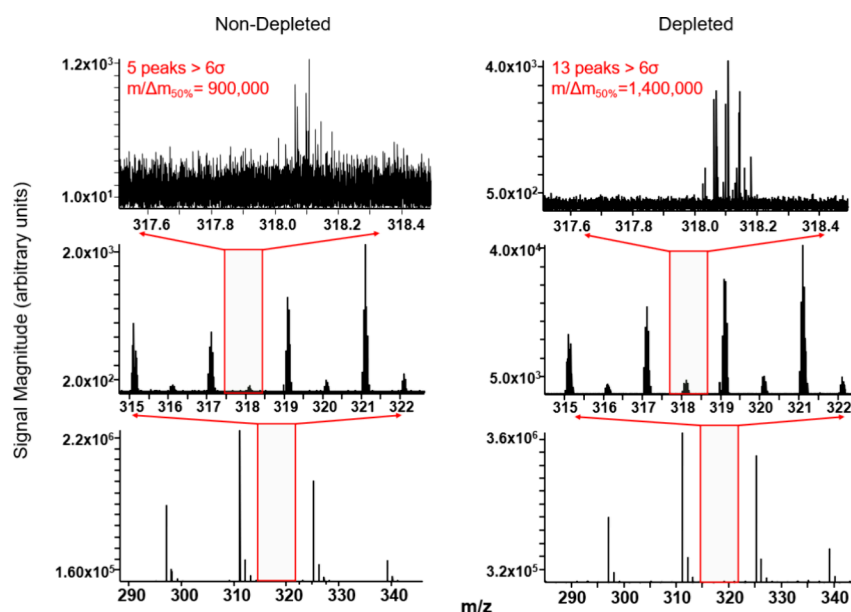


**Figure 3.** Expansion of a single nominal  $m/z$  to display the underlying spectral complexity in the absence (left) and presence (right) of a chemical noise depletion waveform. The observed number of peaks increases from 5 peaks to 13 peaks in the top zoom insets. Further, the average resolving power for the detected peaks is improved from 900 000 to 1 400 000.

spectrometer. Spectral regions of the frequency domain which exhibit nonzero magnitude impart kinetic excitation to ions entering the ion trap which are in resonance. This kinetic excitation results in ejection of these ions from the linear RF ion trap, forming the basis of the waveform depletion strategy. Regions highlighted where zero magnitude is observed (except for some small discrete electronic noise) are intended to allow desired analyte ions to remain stably trapped. The synthesis of these waveforms is completely customizable based upon initial empirical observations of each sample. Currently, the approach has been developed to support the depletion of up to 10 independent  $m/z$  values. Often contamination is presented in the form of a polymeric series in which each contaminant peak differs by a discrete repeat unit (ex. polyethylene glycol; PEG  $\Delta m/z = 44$  Da), which makes it possible to recognize and target these species using the ion depletion waveform technique.

#### Waveform Depletion Increases Peak Assignments.

Figure 2 shows broadband negative ESI 21 T FT-ICR mass spectra for a DOM sample without depletion (top) and with depletion applied at  $m/z$  297.08, 311.08, 325.08, 339.08 across a 5 Da width (bottom) as demonstrated in the waveform shown in Figure 1. These contaminants are present as a polymeric series with a delta  $m/z \sim 14$  Th corresponding to  $\text{CH}_2$  additions to the aliphatic tail of these detergent compounds. Table S1 shows a list of  $\text{O}_3\text{S}$  contaminant peaks detected in the field blank, with Figure S1 showing DBE versus carbon number images for the  $\text{O}_3\text{S}$  class. Chemical noise peaks that correspond to linear alkylbenzenesulfonates (Figure S1) can be observed at  $\sim 10$  times higher signal magnitude compared to the DOM distribution between  $m/z$  185–275\*, with the molecular weight distribution of both spectra (with and without depletion) from  $m/z$  150–900. Without depletion, approximately 22 000 peaks are detected and assigned elemental compositions (89 ppb rms error). With chemical noise depletion applied, approximately 31 000 peaks are assigned, which is an increase of  $\sim 40\%$ .

#### Signal-to-Noise Ratio and Spectral Complexity Improves with Waveform Depletion.

Figure 3 further highlights the improvement in signal-to-noise ratio and resolving power in another DOM sample that contains  $\text{O}_3\text{S}$  contaminant species that are several orders of magnitude higher in abundance than the DOM analyte species (the broadband mass spectrum is shown in Figure S2). The number of peaks detected per nominal  $m/z$  is improved, as shown for selected regions of the spectrum in Figure 3. In the case where ion depletion was not applied (Figure 3a), 5 peaks were observed at a limit of detection of  $6\sigma$ , whereas 13 peaks were detected at the same threshold with the depletion enabled (Figure 3b). This illustrates direct improvement in spectral complexity elicited through ion depletion observed over this region of the spectrum. Minimizing contaminant ions improves signal-to-noise ratio for all observed species, and many additional analyte species are observed above the limit of detection. In addition, the resolving power at  $m/z$  300 improves by  $\sim 35\%$  with depletion enabled. Across the same mass region, the spectrum with waveform depletion more than doubled the number of peaks per nominal mass and resulted in higher resolving power, thus allowing for subsequent detection and elemental composition assignment. The improved S/N, resolving power, and mass spectral complexity with waveform depletion reveals molecular compositional information undetectable in the presence of chemical contamination.

#### Increased Compositional Coverage with Waveform Depletion.

Figure 4 shows van Krevelen diagrams (H/C ratio versus O/C ratio)<sup>26,27</sup> calculated from neutral elemental compositions derived from negative-ion ESI FT-ICR MS without (left) and with (right) depletion waveform applied. Each van Krevelen diagram is composed of molecular formulas unique to the mass spectrum collected without and with application of the ion depletion waveform. Furthermore, Figure 4 highlights the increased compositional range of species detectable only in the depleted spectrum, with 3655 unique peaks (57 ppb rms error) identified in the depleted spectrum across a wide range of H/C (0.5–2.0) and O/C

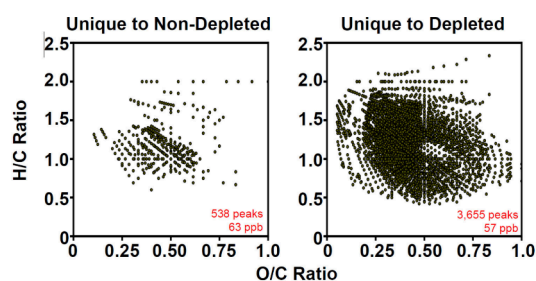


**Figure 4.** van Krevelen diagram of H:C ratio versus O:C ratio calculated from neutral elemental compositions derived from Negative ESI FT-ICR MS without (A) and with (B) a chemical noise depletion waveform applied. Each van Krevelen image contains only elemental compositions derived from mass-to-charge ratios that are unique to each mass spectrum. 538 peaks are unique to the nondepleted sample, compared to 3655 peaks unique to the depleted sample.

(0.1–0.8) ratios. This highlights that FT-ICR mass spectral performance enhancement observed through the application of ion depletion waveforms is a global effect that improves detection of ions of *all*  $m/z$  in the sample and is not localized to only the  $m/z$  ranges that are proximal to the depleted contaminant.

Furthermore, **Figure 5** shows a separate surface water sample contaminated with unknown chemical species. Based on blank analysis, the waveform depletion was set to exclude  $m/z$  195.8, 197.8, 199.8, 201.8, and 203.8. Without depletion,  $\sim 15$  000 peaks were assigned (79 ppb RMS error). With waveform depletion enabled, more than twice the number of peaks were assigned (28 044 peaks with 87 ppb RMS error (**Figure 5a**)). In addition, the compositional information recovered from the sample after application of waveform depletion is shown in **Figure 5b**. More than 16 000 unique elemental compositions are detected across a wide range of O/C and H/C ratios that span the entire molecular weight distribution. Importantly, this further highlights the improvement in compositional information achieved with waveform depletion, because the contaminant peaks are outside of the molecular weight distribution

for the majority of the DOM peaks, yet an increase is observed across the entire molecular weight range of the spectrum. Therefore, waveform depletion can be applied to any chemical peaks in a mass spectrum at any  $m/z$  and result in a significant improvement in the data quality and compositional information from samples that cannot be replicated and have been compromised due to chemical contamination from any source.

## CONCLUSION

We have shown that an ion injection waveform can be constructed and applied to a linear ion trap to reduce chemical noise and improve the mass spectral figures of merit in FT-ICR mass spectrometry. Further, gas-phase ion depletion is extensible beyond chemical contaminants. It has also been effective in depletion of the most abundant analytes of complex mixtures, which permits analogous gains in the number of unique species detected. The current implementation of gas-phase ion depletion requires a priori knowledge of the desired  $m/z$  values for depletion. However, this could be implemented data-dependently for real-time benefit. The authors expect this approach to have broad applicability in LC-MS and MALDI-based<sup>28</sup> acquisition in which background ions can dominate the total ion composition. Finally, this approach has been shown to benefit hybrid FT-ICR MS; however, it could be extended to any linear RF hybrid mass spectrometry platform, including an LTQ-Orbitrap or Orbitrap Tribrid instruments.

## ASSOCIATED CONTENT

### Data Availability Statement

All raw mass spectral data can be obtained at the following Open Science Framework project: DOI 10.17605/OSF.IO/SPK2H.

### Supporting Information

The Supporting Information is available free of charge at <https://pubs.acs.org/doi/10.1021/jasms.4c00261>.

A figure and table to support the main text ([PDF](#))

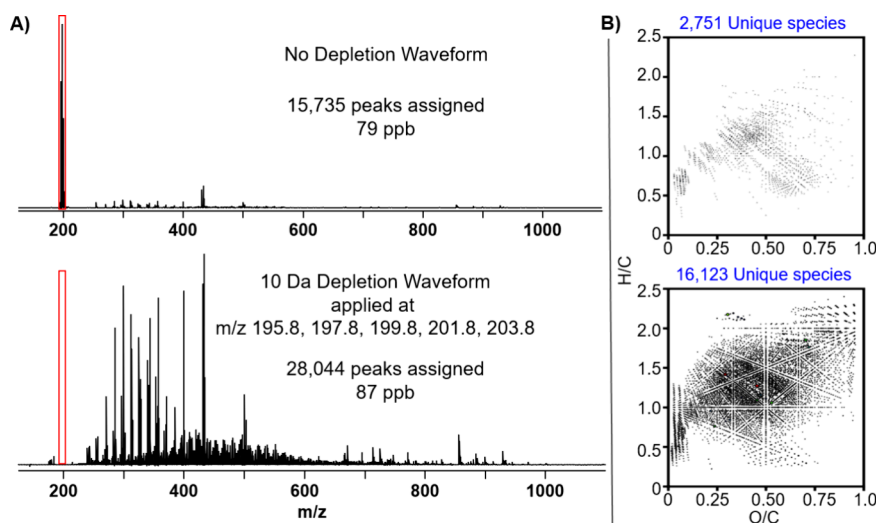


**Figure 5.** (A) Broadband mass spectrum of a groundwater sample contaminated with peaks between  $m/z$  199–203 (top), in which  $\sim 15$  000 peaks were assigned at 79 ppb RMS error without waveform depletion (top) and nearly twice the number of peaks ( $\sim 28$  000) assigned with waveform depletion enabled (bottom) at 87 ppb. (B) van Krevelen diagrams for species unique to the spectrum without depletion (top,  $\sim 2700$  species) and increased detection of more than  $\sim 16$  000 species with waveform depletion enabled (bottom).

## AUTHOR INFORMATION

### Corresponding Author

Chad R. Weisbrod – National High Magnetic Field Laboratory, Florida State University, Tallahassee, Florida 32310-4005, United States; [orcid.org/0000-0001-5324-4525](https://orcid.org/0000-0001-5324-4525); Phone: +1 850 644 9861; Email: [weisbrod@magnet.fsu.edu](mailto:weisbrod@magnet.fsu.edu); Fax: +1 850 644 1366

### Authors

Amy M. McKenna – National High Magnetic Field Laboratory, Florida State University, Tallahassee, Florida 32310-4005, United States; Department of Soil and Crop Sciences, Colorado State University, Fort Collins, Colorado 80521, United States; [orcid.org/0000-0001-7213-521X](https://orcid.org/0000-0001-7213-521X)

Christopher L. Hendrickson – National High Magnetic Field Laboratory, Florida State University, Tallahassee, Florida 32310-4005, United States; [orcid.org/0000-0002-4272-2939](https://orcid.org/0000-0002-4272-2939)

Complete contact information is available at: <https://pubs.acs.org/10.1021/jasms.4c00261>

### Author Contributions

The manuscript was written through contributions of all authors. All authors have given approval to the final version of the manuscript.

### Notes

The authors declare no competing financial interest.

## ACKNOWLEDGMENTS

The authors thank John P. Quinn for design and maintenance of the 21 T instrument, and Gregory T. Blakney for software capabilities, and numerous user groups who have graciously provided access to real-world, challenged, and highly valued samples, including Mengqiang Zhu, Robert G. M. Spencer, Collin P. Ward, Andrew Wozniak, Jason Masoner, and Thomas Borch. This work was performed at the National High Magnetic Field Laboratory, which is supported by National Science Foundation Division of Materials Research and Division of Chemistry through DMR-2128556 and the State of Florida.

## REFERENCES

- (1) Gao, Y.; Wang, W.; He, C.; Fang, Z.; Zhang, Y.; Shi, Q. Fractionation and molecular characterization of natural organic matter (NOM) by solid-phase extraction followed by FT-ICR MS and ion mobility MS. *Anal. Bioanal. Chem.* **2019**, *411*, 6343–6352.
- (2) Phungsai, P.; Kurisu, F.; Kasuga, I.; Furumai, H. Molecular characterization of low molecular weight dissolved organic matter in water reclamation processes using Orbitrap mass spectrometry. *Water Res.* **2016**, *100*, 526–536.
- (3) Song, G.; Mesfiou, R.; Dotson, A.; Westerhoff, P.; Hatcher, P. G. Sulfur-containing molecules observed in hydrophobic and amphiphilic fractions of dissolved organic matter by Fourier transform ion cyclotron resonance mass spectrometry. In *Functions of Natural Organic Matter in Changing Environments*; Xu, J., Ed.; Springer Science+Business Media: Dordrecht, 2013.
- (4) Derrien, M.; Lee, Y. K.; Hur, J. Comparing the spectroscopic and molecular characteristics of different dissolved organic matter fractions isolated by hydrophobic and anionic exchange resins using fluorescence spectroscopy and FT-ICR-MS. *Water* **2017**, *9* (8), 555.
- (5) Ye, Q.; Zhang, Z.-T.; Liu, Y.-C.; Wang, Y.-H.; Zhang, S.; He, C.; Shi, Q.; Zeng, H.-X.; Wang, J.-J. Spectroscopic and molecular-level characteristics of dissolved organic matter in a highly polluted urban river in South China. *ACS Earth Space Chem.* **2019**, *3*, 2033–2044.

- (6) He, D.; He, C.; Li, P.; Zhang, X.; Shi, Q.; Sun, Y. Optical and molecular signatures of dissolved organic matter reflect anthropogenic influence in a coastal river, Northeast China. *J. Environ. Qual.* **2019**, *48* (3), 603–613.

- (7) Gonsior, M.; Zwartjes, M.; Cooper, W. J.; Song, W.; Ishida, K.; Tseng, L. Y.; Jeung, M. K.; Rosso, D.; Hertkorn, N.; Schmitt-Kopplin, P. Molecular characterization of effluent organic matter identified by ultrahigh resolution mass spectrometry. *Water Res.* **2011**, *45* (9), 2943–2953.

- (8) McLuckey, S. A.; Goeringer, D. E.; Glish, G. L. Selective Ion Isolation/Rejection Over a Broad Mass Range in the Quadrupole Ion Trap. *J. Am. Soc. Mass Spectrom.* **1991**, *2* (1), 11–21.

- (9) Goeringer, D. E.; Asano, K. G.; McLuckey, S. A.; et al. Filtered Noise Field Signals for Mass-Selective Accumulation of Externally Formed Ions in a Quadrupole Ion Trap. *Anal. Chem.* **1994**, *66*, 313–318.

- (10) Bruce, J. E.; Anderson, G. A.; Smith, R. D. Colored noise waveforms and quadrupole excitation for the dynamic range expansion of Fourier transform ion cyclotron resonance mass spectrometry. *Anal. Chem.* **1996**, *68* (3), 534–541.

- (11) Belov, M. E.; Anderson, G. A.; Angell, N. H.; Shen, Y.; Tolic, N.; Udseth, H. R.; Smith, R. D. Dynamic range expansion applied to mass spectrometry based on data-dependent selective ion ejection in capillary liquid chromatography Fourier transform ion cyclotron resonance for enhanced proteome characterization. *Anal. Chem.* **2001**, *73* (21), 5052–5060.

- (12) Dittmar, T.; Koch, B.; Hertkorn, N.; Kattner, G. A simple and efficient method for the solid-phase extraction of dissolved organic matter (SPE-DOM) from seawater. *Limnol. Oceanogr. Method.* **2008**, *6*, 230–235.

- (13) Emmett, M. R.; White, F. M.; Hendrickson, C. L.; Shi, S. D.-H.; Marshall, A. G. Application of micro-electrospray liquid chromatography techniques to FT-ICR MS to enable high-sensitivity biological analysis. *J. Am. Soc. Mass Spectrom.* **1998**, *9* (4), 333–340.

- (14) Hendrickson, C. L.; Quinn, J. P.; Kaiser, N. K.; Smith, D. F.; Blakney, G. T.; Chen, T.; Marshall, A. G.; Weisbrod, C. R.; Beu, S. C. 21 T Fourier transform ion cyclotron resonance mass spectrometer: A national resource for ultrahigh resolution mass analysis. *J. Am. Soc. Mass Spectrom.* **2015**, *26*, 1626–1632.

- (15) Smith, D. F.; Podgorski, D. C.; Rodgers, R. P.; Blakney, G. T.; Hendrickson, C. L. 21 T FT-ICR mass spectrometer for ultrahigh resolution analysis of complex organic mixtures. *Anal. Chem.* **2018**, *90* (3), 2041–2047.

- (16) Kaiser, N. K.; Savory, J. J.; Hendrickson, C. L. Controlled ion ejection from an external trap for extended  $m/z$  range in FT-ICR mass spectrometry. *J. Am. Soc. Mass Spectrom.* **2014**, *25*, 943–949.

- (17) Kaiser, N. K.; McKenna, A. M.; Savory, J. J.; Hendrickson, C. L.; Marshall, A. G. Tailored ion radius distribution for increased dynamic range in FT-ICR mass analysis of complex mixtures. *Anal. Chem.* **2013**, *85* (1), 265–272.

- (18) Chen, T.; Beu, S. C.; Kaiser, N. K.; Hendrickson, C. L. Note: Optimized circuit for excitation and detection with one pair of electrodes for improved Fourier transform ion cyclotron resonance mass spectrometry. *Rev. Sci. Instrum.* **2014**, *85* (6), 0666107/1–0666107/3.

- (19) Boldin, I. A.; Nikolaev, E. N. Fourier transform ion cyclotron resonance cell with dynamic harmonization of the electric field in the whole volume by shaping of the excitation and detection electrode assembly. *Rapid Commun. Mass Spectrom.* **2011**, *25* (1), 122–126.

- (20) Kaiser, N. K.; Quinn, J. P.; Blakney, G. T.; Hendrickson, C. L.; Marshall, A. G. A Novel 9.4 T FT ICR mass spectrometer with improved sensitivity, mass resolution, and mass range. *J. Am. Soc. Mass Spectrom.* **2011**, *22* (8), 1343–1351.

- (21) Blakney, G. T.; Hendrickson, C. L.; Marshall, A. G. Predator data station: A fast data acquisition system for advanced FT-ICR MS experiments. *Int. J. Mass Spectrom.* **2011**, *306* (2–3), 246–252.

- (22) Xian, F.; Hendrickson, C. L.; Blakney, G. T.; Beu, S. C.; Marshall, A. G. Automated Broadband Phase Correction of Fourier

Transform Ion Cyclotron Resonance Mass Spectra. *Anal. Chem.* **2010**, *82* (21), 8807–8812.

(23) Savory, J. J.; Kaiser, N. K.; McKenna, A. M.; Xian, F.; Blakney, G. T.; Rodgers, R. P.; Hendrickson, C. L.; Marshall, A. G. Parts-Per-Billion Fourier transform ion cyclotron resonance mass measurement accuracy with a "Walking" calibration equation. *Anal. Chem.* **2011**, *83* (5), 1732–1736.

(24) McLafferty, F. W.; Turecek, F. *Interpretation of Mass Spectra*, 4th ed.; University Science Books: Mill Valley, CA, 1993.

(25) Corilo, Y. E. *PetroOrg. Software*; Florida State University, Omics LLC: Tallahassee, FL, 2014.

(26) van Krevelen, D. W. Graphical-statistical method for the study of structure and reaction processes of coal. *Fuel* **1950**, *29*, 269–284.

(27) Kim, S.; Kramer, R. W.; Hatcher, P. G. Graphical method for analysis of ultrahigh-resolution broadband mass spectra of natural organic matter, the van Krevelen diagram. *Anal. Chem.* **2003**, *75* (20), 5336–5344.

(28) Prentice, B. M.; Ryan, D. J.; Grove, K. J.; Cornett, D. S.; Caprioli, R. M.; Spraggins, J. M. Dynamic Range Expansion by Gas-Phase Ion Fractionation and Enrichment for Imaging Mass Spectrometry. *Anal. Chem.* **2020**, *92*, 13092–13100.